



## Solar photocatalytic activity of sol–gel prepared Ag-doped ZnO thin films

Mohamed I. Badawy<sup>a</sup>, F.A. Mahmoud<sup>b</sup>, Ahmed A. Abdel-Khalek<sup>c</sup>, Tarek A. Gad-Allah<sup>a</sup>, A.A. Abdel Samad<sup>a,\*</sup>

<sup>a</sup>Water Pollution Research Department, National Research Centre (NRC), El Buhouth St., Dokki, Cairo, Egypt  
Tel. 0020119590419; email: Ahmedgera@hotmail.com

<sup>b</sup>Solid State Physics Department, National Research Centre (NRC), El Buhouth St., Dokki, Cairo, Egypt

<sup>c</sup>Faculty of Science, Chemistry Department, Beni-suef University, Slah Salem St., Beni-suef, Egypt

Received 28 February 2012; Accepted 3 April 2013

---

### ABSTRACT

Pure and silver doped ZnO thin films over glass substrate were prepared by sol–gel spin-coating method. Prepared films were calcined at different temperatures. X-ray diffraction and UV–Vis spectroscopy were used to characterize the prepared samples. The photocatalytic activity under solar irradiation of the prepared thin films was tested for the degradation of three azo reactive dyes namely Reactive Red 195, Reactive yellow 145 and Reactive orange 122 as an organic pollutant. 6 wt.% Ag doping ratio showed the highest photocatalytic activity. Various operational parameters such as pH of the solution and initial concentration of the dye have been investigated.

*Keywords:* ZnO; Thin film; Ag; Doping; Photocatalysis; Solar light; RR195; RY145; RO122

---

### 1. Introduction

The textile industry has become very commercialized and has contributed positively to the economic growth of Egypt. The total water used by the textile industry sector is estimated to be 4–5% (approximately 250 Mm<sup>3</sup>/year) of Egypt's industry water demand [1]. Wastewaters produced from textile and other dyestuff industrial processes contain large quantities of azo dyes constituting a significant portion and having the least desirable consequences in terms of surrounding ecosystems. They are also resistant to aerobic degradation and under anaerobic conditions they can be reduced to potentially carcinogenic

aromatic amines [2]. In an USEPA study, 11 of the 18 azo dyes passed through activated sludge process untreated [3]. While physical processes, such as coagulation and adsorption, merely transfer the pollutant from wastewater to other media and cause secondary pollution. In the near future, advanced oxidation processes (AOPs) may become the most widely used water treatment technologies for organic pollutants not treatable by conventional techniques, due to their high chemical stability and/or low biodegradability [4–6]. These processes involve generation and subsequent reaction of hydroxyl radicals (OH<sup>\*</sup>), which are one of the most powerful oxidizing species.

Heterogeneous photocatalysis is a promising new alternative method among AOPs which generally includes UV/H<sub>2</sub>O<sub>2</sub>, UV/O<sub>3</sub>, or UV/Fenton's reagent

---

\*Corresponding author.

for oxidative removal of organic chemicals [7,8]. In recent years, interest has been focused on the use of semiconductor materials as photocatalysts for the removal of organic and inorganic species from aqueous or gas phase. This method has been suggested in environmental protection due to its ability to oxidize the organic and inorganic substrates [9]. Among the various semiconductors employed,  $\text{TiO}_2$  and  $\text{ZnO}$  are known good photocatalysts for the degradation of several environmental contaminants [10–14] due to their high photosensitivity, stability, and large band gap [15].  $\text{ZnO}$  and  $\text{TiO}_2$  have similar band-gap energies around 3.2 eV [16]. When a semiconductor absorbs a photon of energy greater than or equal to the band-gap energy, an electron may be promoted from the valence band to the conduction band, leaving behind an electron vacancy or “hole” in the valence band. If charge separation is maintained, the electron and hole may migrate to the catalyst surface, where they participate in redox reactions with adsorbed species [16,17].

Lower cost and better performance of  $\text{ZnO}$  in the degradation of organic molecules in both acidic and basic medium have stimulated many researchers to further explore the properties of this oxide in many photocatalytic reactions. Some studies have also confirmed that  $\text{ZnO}$  exhibits better photocatalytic efficiency than  $\text{TiO}_2$  [15,18–20] due to its higher efficiency of generation, mobility, and separation of photo-induced electrons and holes [21].

Despite the positive attributes of photocatalysts, there are two main drawbacks associated with them, (i) charge carrier recombination occurs within nanoseconds [22,23] and (ii) the band-edge absorption threshold does not allow the utilization of visible light [24] because only 5% of the solar energy in the ultraviolet range is capable of activating the photocatalytic reaction. To use the solar energy effectively, it is essential to extend the absorption spectrum of the semiconductor into the visible light region, where a much higher proportion (45%) of the solar energy may be used [25]. Many methods were used for this purpose such as modification of  $\text{ZnO}$  by addition of another semiconductor, dye sensitization, and metal or nonmetal doping. In fact, metallic silver is a significant visible light photosensitizer, which is stable and nontoxic compared with dye photosensitizer. Ag is also relatively cheap; thus, Ag modification is of great significance for industrial practice. This study is to enhance the photocatalytic activity of  $\text{ZnO}$  thin films by silver doping using sol–gel technique under solar irradiation. Effect of different operational conditions on the degradation of three azo dyes (RR195, RY145, and RO122) has been investigated.

## 2. Experimental

### 2.1. Materials

All chemicals were reagent grade and were used without further purification. Zinc acetate dehydrate ( $\text{Zn}(\text{CH}_3\text{COO})_2 \cdot 2\text{H}_2\text{O}$ ) CAS Number 5970-45-6 as a precursor of  $\text{ZnO}$ , Isopropanol ( $(\text{CH}_3)_2\text{CHOH}$ ) CAS Number 67-63-0, and Diethanolamine ( $(\text{CH}_2\text{CH}_2\text{OH})_2\text{NH}$ ) (DEA) CAS Number 111-42-2 as a solvent and stabilizer, respectively, were purchased from Sigma Aldrich company. The dyes used (RO122, RY145, and RR195) were kindly supplied by the local factory for dyes. NaOH or HCl solutions were used for pH adjustment. Double-distilled water was used throughout this study for the preparation of dyes solutions.

### 2.2. Synthesis of $\text{ZnO}$ and Ag-doped $\text{ZnO}$ thin films

The key to obtain good quality film using sol–gel spin coating method is the preparation of a clear, transparent, and homogenous solution. Sol solution was prepared according to [26] with slight modifications. In this method, the molar ratio of DEA to zinc acetate dehydrate was maintained at 1.0 and the concentration of zinc acetate dehydrate was 0.4 M. The sol solution was prepared using the following procedure: zinc acetate dihydrate (0.4 M) was first dissolved in appropriated volume of isopropanol and then diethanolamine was added under continuous stirring in order to obtain a clear solution. In case of Ag-doped  $\text{ZnO}$  films, isopropanol solution containing silver nitrate ( $\text{AgNO}_3$ ) was mixed with the clear solution of zinc acetate dihydrate in order to yield 2–10% Ag/Zn weight ratios. Undoped and silver-doped  $\text{ZnO}$  thin films were deposited by sol–gel spin coating method onto glass substrates. At first, glass substrate was pre-cleaned with detergent, ethanol, acetone and finally with distilled water for 10 min, in Bandelin Sonorex RK100, and then dried. For film formation, the sol solution was dropped within 30 s onto a glass substrate rotating at 2000 rpm using the spin coater. The spin-coating deposition was performed at room temperature. Films were then dried at 100 °C for 10 min in order to remove the solvent. This procedure was repeated seven times to obtain homogeneous coating. Finally, all prepared films were annealed in air atmosphere at 350 and 450 °C for 1 h in tubular furnace.

### 2.3. Characterization of prepared films

The X-ray diffraction (XRD) analysis of the samples was performed at room temperature by diffractometer (Philips diffract meter (40 kV, 30 mA) with nickel filter and copper radiation.

The optical transmittance and reflectance of the films were performed by (JASCO V500, Japan) UV–VIS spectrophotometer.

#### 2.4. Photocatalytic measurement

Photocatalytic efficiency of the prepared films was evaluated by the decolorization of three reactive azo dyes; reactive red 195, reactive yellow 145, and reactive orange 122. Seventy-five milliliters of 10 ppm dye solution was placed in a glass Petri dish. A catalyst of rectangular geometry  $1.2 \times 2.6$  cm was immersed in the dye solution. Simulate solar irradiation was delivered by (HQI-T 400 W/DayLight OSRAM Germany). The luminous flux of irradiation was 20,000 lm with luminous efficacy of 82 lm/W. The distance between the surface of dye solution and the lamp was 15 cm. Prior to starting irradiation, the dye solution was allowed to be in contact with photocatalyst for 30 min in dark to allow the adsorption–desorption equilibrium on the photocatalyst surface. Then, the lamp was switched on to start photodegradation of dyes. Definite quantities of aliquot were collected at regular intervals under dark and irradiation conditions. Color fading was monitored by measuring the absorbance UV–vis spectrophotometer (JASCO V500, Japan).

### 3. Results and discussion

#### 3.1. Characterization of prepared films

##### 3.1.1. X-ray diffraction

In order to investigate the effect of silver doping on the crystal structure of ZnO, XRD measurements have been taken in  $2\theta$  range of  $20$ – $70^\circ$  for the pure

and Ag–ZnO thin films. Fig. 1 shows the XRD patterns for pure and silver-doped ZnO thin films calcined at 350 and 450 °C. All deposited films were polycrystalline with a hexagonal wurtzite structure, under the investigated calcination temperatures. Also, it is remarkable that crystallinity of ZnO was enhanced by the addition of Ag and by increasing the calcination temperature. The crystallinity of the films begin to improve by addition of 2 wt.% Ag, but this improvement disappears at 4 wt.% Ag because in the case of 4%, the silver peak begins to appear and this may change the crystal properties of ZnO crystal. The films that were treated at 350 °C calcination temperature showed no preferred orientations of ZnO plane, while in case of 450 °C calcination temperature 002 plane appeared as the preferred orientation.

Ag can be incorporated in ZnO system, either as a substitute for  $\text{Zn}^{2+}$  or as an interstitial atom. Usually peak shift in XRD pattern is observed when  $\text{Zn}^{2+}$  is substituted by Ag atom. The absence of this shift in case of prepared Ag/ZnO films revealed that Ag particles are separated from the grain boundaries of ZnO crystallites rather than going into the lattice of ZnO, or only an insignificant quantity may be going to the substitutional Zn site and other quantity agglomerates on the surface. The increase in peak intensity of Ag with the increase in silver content also supports this explanation. The same result was reported by Zhang and Mu [27].

##### 3.1.2. Optical studies

UV–vis transmission spectra provide useful information about the band gap of semiconductors. The recorded spectra of Ag/ZnO thin films deposited on

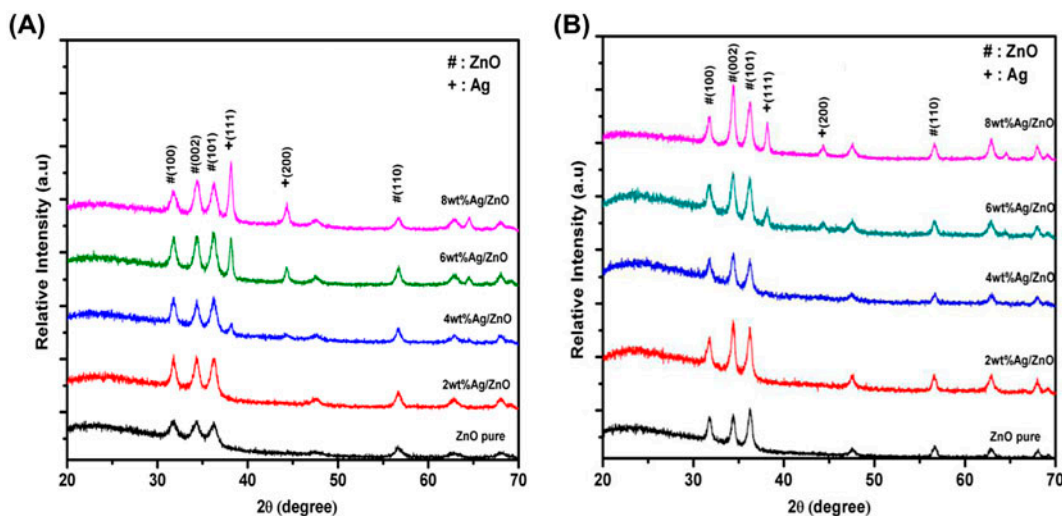


Fig. 1. XRD patterns of the Ag/ZnO films of various silver contents calcined at (A) 350 °C and (B) 450 °C for 1 h.

glass substrate in the range of 350–800 nm are shown in Fig. 2. The transmittance decreased sharply near the ultraviolet region due to the band-gap absorption. The spectra also clearly exhibited a shift in band edge, with the variation of Ag content. Transmittance of Ag/ZnO films in the visible region shrinks with increase in the calcination temperature, from 350 to 450 °C, and the silver content. This shrinkage in the transmittance values of the Ag/ZnO thin films may be due to the grain boundary scattering and the absorption of the visible light by surface plasmon resonance (SPR) resulted from Ag nanoparticles.

At the films calcined at 350 °C, the SPR peak of Ag doping observed up to 6 wt.% doping. However, by increasing the calcinations to 450 °C, we observe no more enhancement in the SPR peak. Tarwal and Patil

also observed the effect of SPR phenomena at the optical properties of Ag/ZnO thin film prepared by spray pyrolysis [28].

The absorbance coefficient ( $\alpha$ ) was calculated from the raw absorption data to obtain the optical band gap,  $E_g$ .  $E_g$  is the separation between the bottom of the conduction band and the top of the valence band. Fig. 3 shows variation of  $(\alpha h\nu)^2$  as a function of photon energy ( $h\nu$ ). Band-gap value was determined by extrapolation of the linear portion of Fig. 3.  $E_g$  was found to be 3.33 eV for pure ZnO thin film, which is in agreement with the formerly reported value for wurtzite-structured transparent ZnO film [29]. The calculated  $E_g$  values of the films was narrowed with increase in Ag contents, which decreased from 3.33 to 3.207 eV when calcination temperature was 350 °C and

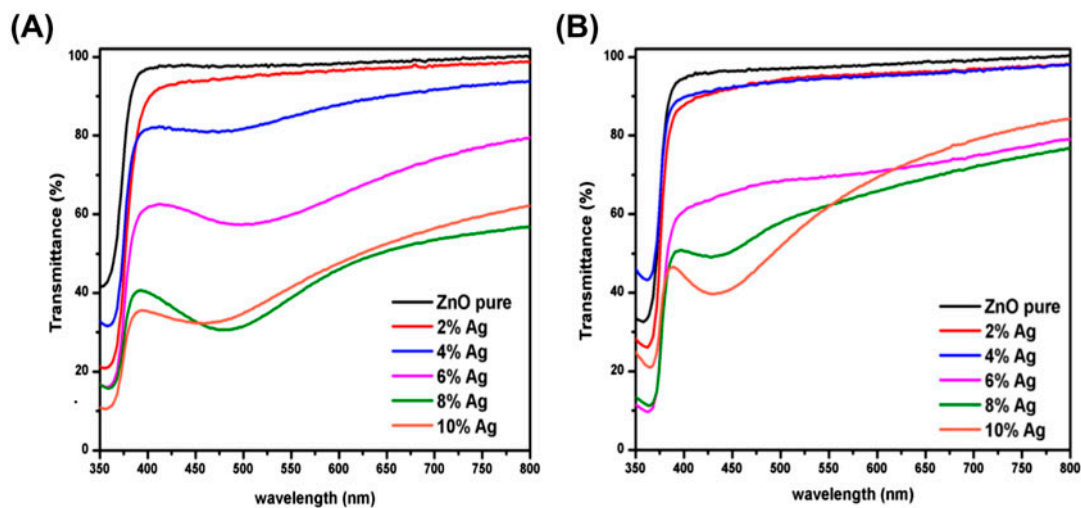


Fig. 2. Optical transmittance of Ag/ZnO thin films calcined (A) at 350 °C and (B) at 450 °C.

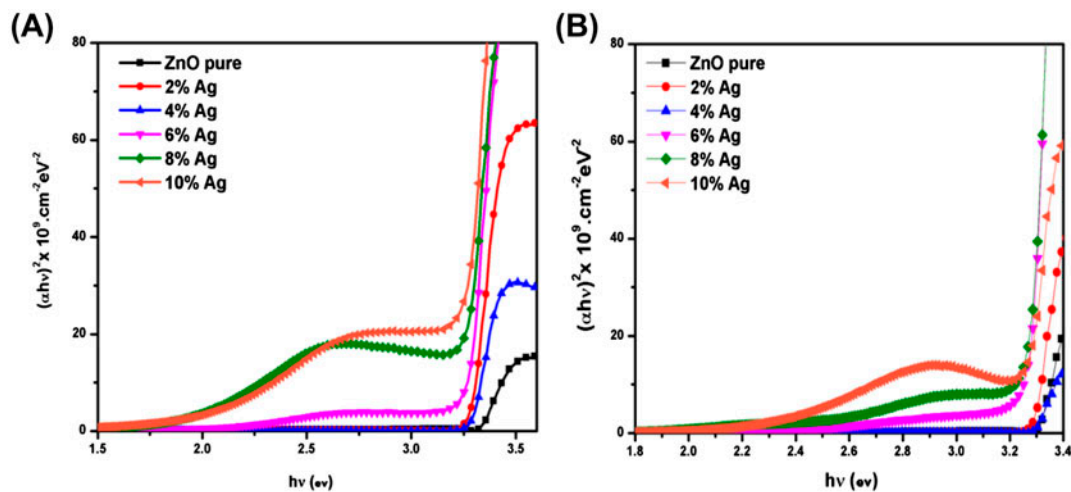


Fig. 3.  $(\alpha h\nu)^2$  vs.  $h\nu$  of pure and Ag-doped ZnO thin films calcined at (A) at 350 °C and (B) at 450 °C.

from 3.30 to 3.19 eV when the calcination temperature was raised to 450°C. The narrowing of band gap by more Ag contents reveals that the prepared films can be activated under visible light irradiation. However, no more change in the  $E_g$  values with changing calcinations temperature, the films calcinated at 450°C show more efficiency in the photocatalytic activity; this may be related to the enhancement in the crystallinity of these films.

### 3.2. Photocatalytic activity

An important aim of this study involves the examination of photocatalytic activity of Ag/ZnO thin films under simulated solar irradiation. Three reactive dyes (Reactive Red 195, Reactive Yellow 145, and Reactive Orange 122) were selected as representatives of organic pollutants to evaluate the photocatalytic performance of Ag/ZnO thin films. Prior to investigating reaction conditions, it was confirmed that the three dyes are resistant to direct photolysis, i.e. photodegradation in the absence of photocatalyst. According to a number of researches [30,31], the influence of the initial concentration on the solute to the photocatalytic degradation rate of most organic compounds is described by a pseudo-first kinetic order.

The same result we had where Photocatalytic reaction of each dye by Ag/ZnO photocatalyst was found to obey pseudo-first-order kinetics (Eq. 1).

$$-\frac{dC}{dt} = k[C_{dye}] \quad (1)$$

where  $k$  is the pseudo-first-order rate constant. Integration of Eq. (1) gives Eq. (2)

$$\ln \left[ \frac{C_0}{C} \right] = kt \quad (2)$$

where  $C_0$  is the initial concentration of the dye and  $C$  is the concentration at time " $t$ ".  $k$  was calculated using Eq. (2) and was used for the determination of optimum reaction conditions.

#### 3.2.1. Effect of Ag content

Fig. 4 reflects the effect of Ag content on the rate constant of photocatalytic degradation of studied dyes. The result illustrated that the photodegradation rate constant of the three dyes was enhanced by the addition of Ag content up to 6 wt.% of Ag, after which a decline in rate constant was observed. Thus, the optimum doping ratio was considered to be 6 wt.% of

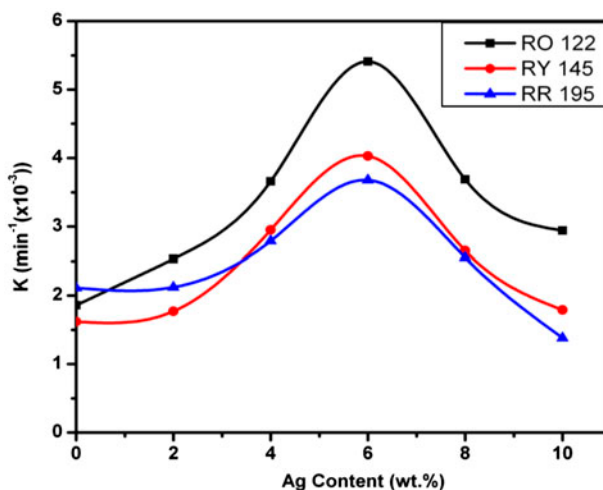


Fig. 4. Rate constant of photocatalytic degradation RR195, RY145, and RO122, catalyst dose: glass slide (2.5 cm × 1 cm), [dye]=10 mg/L, pH=7, calcination temperature=450°C, reaction time=180 min.

Ag, which is in agreement with previous studies results reported by Zhang [27].

The improved activity of Ag/ZnO may be due to better charge separation by Ag atoms. Besides, the incorporation of noble metal onto the ZnO surface increases the rate of electron transfer to dissolved oxygen. On the other hand, silver particles may act as recombination centers at high silver content i.e. prevent the recombination of photogenerated electron-hole, that recombination is caused by the electrostatic attraction of negatively charged silver and positively charged holes [32].

#### 3.2.2. Effect of dye concentration

The effect of initial concentration of the dye on the rate of photocatalytic degradation was performed by varying the initial dye concentration from 10 to 25 mg/L at constant area of the catalyst (2.5 cm × 1 cm).

It is obvious from Fig. 5 that the rate increases with decreasing dye concentration. In general, the rate of degradation relates to the formation of  $\cdot\text{OH}$  radical which is the critical species in the degradation process, the equilibrium adsorption of reactants on the catalyst surface and to the rate of reaction of  $\cdot\text{OH}$  radicals with other chemicals. Matthews [33] suggested that the photocatalytic degradation of aromatic compounds is through hydroxylation of hydroxyl radicals while Okamoto et al. [13] pointed out that the rate-determining step of the reaction may be the formation of  $\cdot\text{OH}$  since they react very rapidly with aromatic ring compounds.

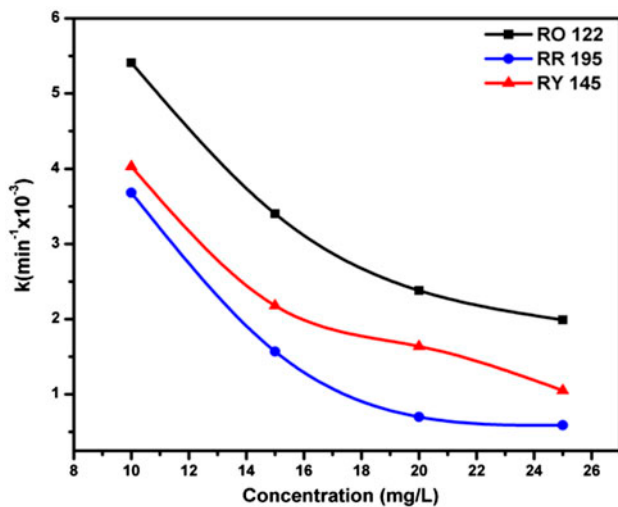


Fig. 5. Rate constant of photocatalytic degradation of RR195, RY145, and RO122 as a function of dye concentration, Ag content=6 wt.%, catalyst dose: glass slide ( $2.5 \text{ cm} \times 1 \text{ cm}$ ), pH=7, calcination temperature =  $450^\circ \text{C}$ , reaction time = 180 min.

As the initial concentration of dye increases, more and more dye molecules are available, but the number of  $\cdot\text{OH}$  and  $\text{O}_2^{\cdot-}$  radicals formed on the surface of ZnO and the irradiation time are constant. Therefore, relative number of  $\cdot\text{OH}$  and  $\text{O}_2^{\cdot-}$  radicals available for attacking the substrate becomes less in comparison to dye molecules; hence, photodegradation rate decreases with increasing dye concentration. Also, as the concentration of dye increases, the photons get interrupted before they can reach the photocatalyst surface and hence absorption of photons by the photocatalyst decreases, and consequently the photocatalytic degradation rate reduces.

In general, the dependency of photocatalytic reaction rates on the concentration of organic pollutants is well described by the Langmuir–Hinshelwood kinetic model modified to accommodate reactions occurring at a solid–liquid interface [34].

$$\frac{1}{r^0} = \frac{1}{k} + \frac{1}{kKC^0} \quad (3)$$

where  $r$  is the oxidation rate of the reactant ( $\text{mg/L min}^{-1}$ ),  $C$  is the concentration of the reactant ( $\text{mg/L}$ ),  $k$  is the reaction rate constant ( $\text{min}^{-1}$ ), and  $K$  is the adsorption coefficient of the reactant onto the catalyst particles ( $\text{L/mg}$ ). Fig. 6 was obtained by plotting reciprocal of the initial rate ( $1/r$ ) against reciprocal of the initial concentration ( $1/C$ ). It is clear that the slope of each line in the negative mode, verifying that the amount of adsorbed dye on the surface of catalyst can be neglected, and hence the reaction occurs on the bulk of solution rather than on catalyst surface.

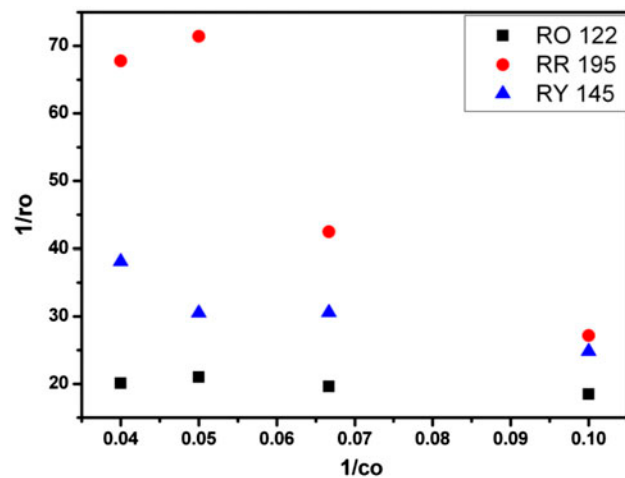


Fig. 6. L-H model verification for photodegradation of RY 145, RR195 and RO122, Ag content=6 wt.%, catalyst dose: glass slide ( $2.5 \text{ cm} \times 1 \text{ cm}$ ), pH=7, calcination temperature =  $450^\circ \text{C}$ , reaction time = 180 min.

### 3.2.3. Effect of pH

The wastewater from textile industries usually has a wide range of pH values. Further, the generation of hydroxyl radicals is also a function of pH. Thus, pH is an important parameter in photocatalytic reactions. Therefore, the degradation of dye was studied at different pH levels ranging from 3 to 11. In all experiments, pH was adjusted by adding appropriate amounts of NaOH or HCl solutions. The change in photodegradation rate constant as a function of pH is shown in Fig. 7. For all dyes, highest photodegradation

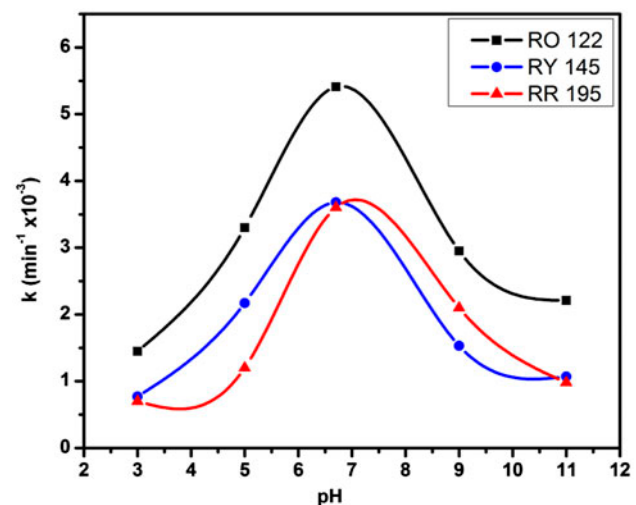


Fig. 7. Rate constant of photocatalytic degradation of RR195, RY145, and RO122 as a function of pH, Ag content=6 wt.%, catalyst dose: glass slide ( $2.5 \text{ cm} \times 1 \text{ cm}$ ), pH=7, calcination temperature =  $450^\circ \text{C}$ , reaction time = 180 min.

rate was observed at natural pH of dyes (7); below or above this value a reduction in rate constant was observed.

The interpretation of pH effect on the efficiency of the photodegradation process is a very difficult task, because three possible reaction mechanisms can contribute to dye degradation, namely, hydroxyl radical attack direct oxidation by the positive hole, and direct reduction by the electron in the conduction band. The importance of each one depends on the substrate nature and pH [35]. The pH affects not only the surface properties of ZnO, but also the dissociation of dyes and formation of hydroxyl radicals.

The point of zero charge (pzc) of ZnO is at pH 9.0  $\pm$  0.3. So, when the solution pH > pH<sub>pzc</sub> (pH > 9), the surface of ZnO is negatively charged [17]. As a result, hydroxyl anions and the dye ions (dye<sup>-</sup>) may be repelled away from the negatively charged ZnO surface. Therefore, the photocatalytic activity of the catalyst reduces at more alkaline medium. At acidic pH range the removal efficiency is at minimum. This may be due to the azo linkage (–N=N–) in our dyes which is particularly susceptible to electrophilic attack by hydroxyl radical. But at low pH, the concentration of H<sup>+</sup> is in excess and H<sup>+</sup> ions interact with azo linkage decreasing the electron densities at azo group. Consequently, the reactivity of hydroxyl radical by electrophilic mechanism decreases [36], though at natural conditions around neutral pH, the equilibrium between the H<sup>+</sup> and OH<sup>-</sup> species give the chance to the hydroxyl radicals to attack the lone pairs of electrons of the azo linkage (–N=N–) easily giving maximum photocatalytic activity.

#### 4. Conclusions

In this study, pure and silver-doped zinc oxide thin films with different wt.% of silver were successfully synthesized by spin-coating sol-gel technique, and the crystal structures of the films were confirmed by the result of XRD. Ag atoms were found to be agglomerated on ZnO film surface, rather than substitute Zn atoms. Study of UV-vis absorption spectra illustrated that Ag-doping reduced the band-gap energy of ZnO, leading to absorption in visible light range. Ag/ZnO films revealed good photocatalytic decolorization of three azo reactive dyes (Reactive Red 195, Reactive yellow 145, and Reactive orange 122) under simulated sunlight. It was found that depositing Ag on ZnO surface boosts its photocatalytic activity and depends on the content of metallic silver in the zinc oxide films and calcinations temperature. The optimal content of Ag was 6 wt.%. Samples

calcined at 450 °C possessed higher activity toward the degradation of the three dyes than those calcined at 350 °C. The highest rate of photodegradation was obtained at natural pH of the studied dyes.

#### References

- [1] SEAM project, guidance manual cleaner production production for textile water and energy conservation, August, 1999.
- [2] W.Z. Tang, H. An, UV/TiO<sub>2</sub> photocatalytic oxidation of commercial dyes in aqueous solutions, *Chemosphere* 31 (1995) 4157–4170.
- [3] G.M. Shaul, T.J. Holdsworth, C.R. Dempsey, K.A. Dostal, Fate of water soluble azo dyes in the activated sludge process, *Chemosphere* 22 (1991) 107–119.
- [4] I.K. Konstantinou, T.A. Albanis, TiO<sub>2</sub>-assisted photocatalytic degradation of azo dyes in aqueous solution: kinetic and mechanistic investigations: A review, *Appl. Catal. B* 49 (2004) 1–14.
- [5] M. Pera-Titus, V. Garca-Molina, M.A. Banos, J. Gimenez, S. Esplugas, Degradation of chlorophenols by means of advanced oxidation processes: A general review, *Appl. Catal. B* 47 (2004) 219–265.
- [6] I. Munoz, J. Rieradevall, F. Torrades, J. Peral, X. Domenech, Environmental assessment of different solar driven advanced oxidation processes, *Sol. Energy* 79 (2005) 369–375.
- [7] P.R. Gogate, A.B. Pandit, A review of imperative technologies for wastewater treatment I: Oxidation technologies at ambient conditions, *Adv. Environ. Res.* 8 (2004) 501–551.
- [8] P.R. Gogate, A.B. Pandit, A review of imperative technologies for wastewater treatment II: Hybrid methods, *Adv. Environ. Res.* 8 (2004) 553–597.
- [9] M.A. Fox, M.T. Dulay, Heterogeneous photocatalysis, *Chem. Rev.* 93 (1993) 341–357.
- [10] S. Sakthivel, B. Neppolian, M. Palanichamy, B. Arabindoo, V. Murugesan, Photocatalytic degradation of leather dye, acid green 16 using ZnO in the slurry and thin film forms, *Indian J. Chem. Technol.* 6 (1999) 161–165.
- [11] S. Sakthivel, B. Neppolian, B. Arabindoo, M. Palanichamy, V. Murugesan, TiO<sub>2</sub> catalysed photodegradation of leather dye acid green 16, *J. Sci. Ind. Res.* 59 (2000) 556–562.
- [12] S. Sakthivel, B. Neppolian, B. Arabindoo, M. Palanichamy, V. Murugesan, Solar photocatalytic degradation of azo dye: Comparison of photocatalytic efficiency of ZnO and TiO<sub>2</sub>, *Sol. Energy Mater. Sol. Cells* 77 (2003) 65–82.
- [13] K.I. Okamoto, Y. Yamamoto, H. Tanaka, M. Tanaka, Heterogeneous photocatalytic decomposition of phenol over TiO<sub>2</sub> powder, *Bull. Chem. Soc. Jpn.* 58 (1985) 2015–2022.
- [14] A. Sharma, P. Rao, R.P. Mathur, S.C. Ametha, Photocatalytic reactions of xylidine ponceau on semiconducting zinc oxide powder, *J. Photochem. Photobiol. A* 86 (1995) 197–200.
- [15] A. Stroyuk, V. Shvalagin, S. Kuchmii, Photochemical synthesis and optical properties of binary and ternary metal-semiconductor composites based on zinc oxide nanoparticles, *J. Photochem. Photobiol. A* 173 (2005) 185–194.
- [16] E. Yassitepe, H.C. Yatmaz, C. Ozturk, K. Ozturk, C. Duran, Photocatalytic efficiency of ZnO plates in degradation of azo dye solution, *J. Photochem. Photobiol. A* 198 (2008) 1–6.
- [17] S.K. Pardeshi, A.B. Patil, Solar photocatalytic degradation of resorcinol a model endocrine disrupter in water using zinc oxide, *J. Hazard. Mater.* 163 (2009) 403–409.
- [18] F. Lu, W.P. Cai, Y.G. Zhang, ZnO hierarchical micro/nanoarchitectures: Solvothermal synthesis and structurally enhanced photocatalytic performance, *Adv. Funct. Mater.* 18 (2008) 1047–1056.
- [19] V. Kandavelu, H. Kastien, K. Ravindranathan Thampi, Photocatalytic degradation of isothiazolin-3-ones in water and emulsion paints containing nanocrystalline TiO<sub>2</sub> and ZnO catalysts, *Appl. Catal. B* 48 (2004) 101–111.

- [20] M.J. Height, S.E. Pratsinis, O. Mekasuwandumrong, P. Praserttham, Ag-ZnO Catalysts for UV-photodegradation of methylene blue, *Appl. Catal. B* 63 (2006) 305–312.
- [21] Y.Z. Li, W. Xie, X.L. Hu, G.F. Shen, X. Zhou, Y. Xiang, X.J. Zhao, P.F. Fang, Comparison of dye photodegradation and its coupling with light-to-electricity conversion over TiO<sub>2</sub> and ZnO, *Langmuir* 26 (2010) 591–597.
- [22] G. Rothenberger, J. Moser, M. Grätzel, N. Serpone, D.K. Sharma, Charge carrier trapping and recombination dynamics in small semiconductor particles, *J. Am. Chem. Soc.* 107 (1985) 8054–8059.
- [23] N. Serpone, E. Pelizzetti, *Photocatalysis: Fundamentals and Applications*, Wiley, New York, 1989.
- [24] N. Serpone, D. Lawless, J. Disdier, J.-M. Herrmann, Spectroscopic, photoconductivity, and photocatalytic studies of TiO<sub>2</sub> colloids: Naked and with the lattice doped with Cr<sup>3+</sup>, Fe<sup>3+</sup>, and V<sup>5+</sup> cations, *Langmuir* 10 (1994) 643–652.
- [25] F. Fang, Q. Li, J. Shang, Enhanced visible-light absorption from Ag<sub>2</sub>O nanoparticles in nitrogen-doped TiO<sub>2</sub> thin films, *Surf. Coat. Technol.* 205 (2011) 2919–2923.
- [26] Y. Kim, W. Tai, S. Shu, Effect of preheating temperature on structural and optical properties of ZnO thin films by sol-gel process, *Thin Solid Films* 491 (2005) 153–160.
- [27] Y. Zhang, J. Mu, One-pot synthesis, photoluminescence, and photocatalysis of Ag/ZnO composites, *J. Colloid Interface Sci.* 309 (2007) 478–484.
- [28] N.L. Tarwal, P.S. Patil, Enhanced photoelectrochemical performance of Ag-ZnO thin films, synthesized by spray pyrolysis technique, *Electrochim. Acta* 56 (2011) 6510–6516.
- [29] M. Izaki, T. Omi, Transparent zinc oxide films chemically prepared from aqueous solution, *J. Electrochem. Soc.* 144 (1997) 3–5.
- [30] O. Mahadwad, P. Parikh, R. Jasra, C. Patil, Immobilized photocatalytic degradation of textile dyes with poly vinyl acetate as a binder, *Int. J. Ind. Eng. Technol.* 4 (2012) 47–59.
- [31] A. Abdelkhalhar, B. Stephan, M. Jean, L. El Kbir, Photocatalytic degradation of azo-dyes reactive black 5 and reactive yellow 145 in water over a newly deposited titanium dioxide, *J. Appl. Catal. B* 57 (2005) 55–62.
- [32] J. Xu, Y. Chang, Y. Zhang, S. Ma, Y. Qu, C. Xu, Effect of silver ions on the structure of ZnO and photocatalytic performance of Ag/ZnO composites, *Appl. Surf. Sci.* 255 (2008) 1996–1999.
- [33] R.W. Matthews, Hydroxylation reactions induced by near-ultraviolet photolysis of aqueous titanium dioxide suspensions, *J. Chem. Soc. Faraday Trans.* 80 (1984) 457–471.
- [34] C. Wang, C. Lee, M. Lyu, L. Juang, Photocatalytic degradation of C.I. basic violet 10 using TiO<sub>2</sub> catalysts supported by Y zeolite: An investigation of the effects of operational parameters, *Dyes Pigm.* 76 (2008) 817–824.
- [35] W. Tang, Z. Zhang, H. An, M. Quintana, D. Torres, TiO<sub>2</sub>/UV photodegradation of azo dyes in aqueous solutions, *Environ. Technol.* 18 (1997) 1–12.
- [36] M. Muruganandham, M. Swaminathan, Photocatalytic decolorisation and degradation of reactive orange 4 by TiO<sub>2</sub>-UV process, *Dyes Pigm.* 68 (2006) 133–141.